Original Research Article

Testing the Shoulder Point Compression Framework on 13 Pairs of Used Athletic Shoes

Taylor A. Mangoba

Manlius Pebble Hill School, 5300 Jamesville Road, DeWitt, NY 13214, United States

ABSTRACT

Athletic-shoe cushioning is commonly characterized by pressing on the heel with a materials-testing machine and extracting descriptors from the resulting force–compression curve. These values are peak compression (PC), foam stiffness over low, mid, and high force ranges, energy absorbed (E_{abs}), and energy return efficiency (η). A recent paper proposed four additional "shoulder point" parameters describing the point of maximum energy absorbed per unit force: the efficiency $(E/F)_{max}$, the force (F_{opt}), the compression (x_{opt}), and the energy absorbed (E_{opt}). The original authors treated all four as independent, but whether they add information beyond the conventional descriptors has not been tested. We tested 13 used pairs of athletic shoes from high-school students on a materials-testing machine and examined the relationships among descriptors using correlation and principal component analysis. Two shoulder point parameters, $(E/F)_{max}$ and x_{opt}, tracked peak compression almost exactly, adding little new information. A third, F_{opt}, was unrelated to every conventional descriptor but closely tracked the foam-stiffening ratio K_{mid}/K_{low}. The fourth, E_{opt}, was well predicted by E_{abs} and F_{opt} together. In this sample the shoulder point framework therefore added one new dimension to the description of cushioning, not four, with F_{opt} the most informative parameter and a possible marker for how cushioning changes as a shoe wears. These findings come from a small convenience sample of 13 pairs of used shoes and should be regarded as preliminary; confirmation in larger and more varied samples is warranted.

Keywords: footwear; compression testing; biomechanics; principal component analysis; materials testing

INTRODUCTION

Athletic shoe midsoles are made of foam, and foam does not compress in a simple way. When a runner's foot lands and presses down on the heel, the foam first compresses easily, then resists more as it gets squeezed, and finally becomes very stiff once the foam cells have collapsed against each other (1). Because the shoe's response changes throughout the compression, a single number like "soft" or "firm" cannot describe how well a shoe cushions an impact. Instead, researchers run a controlled test in which a machine slowly presses down on the heel and records both the force applied and how far the shoe compresses. From the resulting force-compression curve, they typically calculate four kinds of numbers: how much the shoe compresses at a fixed force, how stiff the foam is across one or more force ranges (such as low-load stiffness K_{low}, mid-load stiffness K_{mid}, and high-load stiffness K_{high}), how much energy the shoe absorbs during compression, and how much of that absorbed energy is returned when the force is released (2-4).

Corresponding author: Taylor A. Mangoba, E-mail: tmangoba@me.com.

Accepted July 7, 2026
https://doi.org/10.70251/HYJR2348.44169182

Recent work has proposed an additional set of parameters that describe the moment along the compression curve where the shoe is most efficient at absorbing energy for each newton of force the foot exerts (5). To find this moment, the cumulative energy absorbed up to each point along the curve is divided by the force at that point. The maximum value of this running ratio defines the "shoulder point" and produces four parameters: the peak ratio value itself $(E/F)_{max}$, the force at the shoulder point F_{opt}, the compression at the shoulder point x_{opt}, and the cumulative energy absorbed up to the shoulder point E_{opt}. Fuss *et al.* (5) applied this framework to 112 shoe models and found that shoes with F_{opt} between 0.7 and 2.0 kN matched the typical range of the first vertical force peak that a runner's heel produces on landing. They classified shoes whose F_{opt} fell within this band as well designed for running, and shoes with F_{opt} outside the band as over or under designed.

Whether the four shoulder point parameters carry information that is not already conveyed by conventional descriptors is not obvious. Three of the four parameters, $(E/F)_{max}$, x_{opt}, and E_{opt}, describe either the distance the shoe has compressed or an amount of energy it has absorbed, and conventional measurements already capture both quantities. F_{opt} is the exception. Unlike the other three, F_{opt} is a force, and it locates a specific point along the force axis (the force at which the shoe is most efficient at absorbing energy) that no conventional measurement reports directly. Of the four shoulder point parameters, F_{opt} is therefore the most likely to add genuinely new information, while the other three may overlap with existing descriptors.

A separate reason to test the shoulder point framework on used shoes is that most athletic shoes spend most of their useful life in a partially worn state rather than in new condition. Used shoes show increased midsole stiffness and decreased energy dissipation compared to new ones (6). Whether the four shoulder point parameters keep the same relationships to conventional descriptors when measured on worn athletic shoes has not been directly tested.

It was hypothesized that not all four shoulder point parameters carry independent information beyond conventional compression descriptors, and that the parameters most useful for distinguishing shoes are those that describe the shape of the loading curve rather than its overall magnitude. Three specific predictions followed from this hypothesis. First, the two shoulder point parameters with the same units as a compression distance, $(E/F)_{max}$ and x_{opt}, were predicted to closely match peak compression. Notice that $(E/F)_{max}$ has units of J/N, which simplifies to meters (since J = N·m, the force units cancel leaving a length). Second, F_{opt} was predicted to be the parameter most likely to add new information, since it is the only shoulder point parameter expressed as a force. Third, F_{opt} was predicted to track the foam stiffening ratio K_{mid}/K_{low}, which compares how stiff the foam is in its mid-load range to how stiff it is in its low-load range, on the reasoning that F_{opt} is the force at which energy absorption per unit force is greatest (the shoulder point) beyond which the cushion stiffens into densification and begins to bottom out (5), and that this transition force is set by how quickly the foam stiffens out of its low-load range.

To test these predictions, 13 pairs of used athletic shoes from a convenience sample of high school students were characterized by a materials testing machine, and correlations among the ten compression descriptors (the six conventional descriptors and the four shoulder-point parameters), together with heel height and the foam-stiffening ratio K_{mid}/K_{low} as two additional variables, were computed. Leave one out (LOO) sensitivity analysis was used to check whether each correlation depended on any single shoe in the sample. Principal component analysis of the same ten descriptors (six conventional plus four shoulder-point) was used to identify the largest axes of variation across the sample. The results supported all three predictions, and additionally revealed that E_{opt}, while not predicted to be uniquely informative, shares the F_{opt} defined axis of variation rather than the softness axis defined by peak compression.

METHODS AND MATERIALS

Shoe Sample

Thirteen athletic shoes were obtained from a convenience sample of high school students at the authors' school in DeWitt, NY. Students were asked to bring in a pair of athletic shoes. The 13 shoes represent a range of athletic-shoe categories (running shoes, basketball shoes, lifestyle shoes, and maximalist-cushion shoes) and a range of wear states from very lightly worn to heavily worn. The wear state is treated as descriptive rather than as an independent variable in the analysis. The left and right shoes of each pair were tested separately, and the two sides were then averaged. The unit of analysis throughout this study is therefore the shoe pair, represented by the mean of its left- and right-side measurements; every value reported for a given shoe number (Shoe #1–13) is a left–right pair mean.

The quantitative basis for averaging is described in the Compression Testing section below.

Compression Testing

Each shoe was tested on an electromechanical materials testing system (Instron 5969, Instron, Norwood, MA) using a single symmetric loading and unloading cycle. The shoe was placed sole down on a flat lower plate, and an upper steel cylinder was driven downward onto the shoe from above. A 76 mm (3 in) diameter steel ball weighing approximately 1.8 kg was placed inside the heel of the shoe to focus the load on the heel cushion and to prevent the midsole from being pinched at the edge of the cylinder. The upper cylinder moved downward at 600 mm per minute until the force reached 4,500 N, at which point its direction was reversed at the same speed until the force returned to approximately zero. This completed one full load and unload cycle. The loading and unloading rates were matched because midsole foams are viscoelastic, meaning their apparent stiffness depends on how fast they are compressed. Thus, keeping the rate constant ensured that any gap between the loading and unloading curves reflected the foam's behavior rather than a difference in test speed (3, 4).

The left and right shoes of each pair were tested separately, and the two force–compression loops averaged to give the values reported for that pair. The two sides are separate used shoes worn on opposite feet, not repeat measurements of one specimen, so some between-side difference is expected on physical grounds since midsole mechanical properties change with use (6). Also, the two feet load a shoe differently, hence differences between the left and right shoe are to be expected rather than an indication of a measurement problem. Averaging reflects that the pair, not the individual shoe, is the unit of analysis. Nevertheless, between-side agreement was quantified across the 13 pairs, for every descriptor, by the mean absolute percent difference between sides and by a single-measure, absolute-agreement intraclass correlation coefficient (ICC(2,1) in the Shrout–Fleiss scheme, (7)), which reflects how closely the left and right values of a pair coincide rather than how well they correlate. Left-right agreement was closest for peak compression and x_{opt} (mean difference ≈4–5%, ICC ≥ 0.96), with the remaining showing larger differences (8–18%, ICC 0.44–0.94). The lowest shoulder-point values, for F_{opt} and E_{opt}, arise almost entirely from Shoe #1. Excluding that pair raises both to ICC ≥ 0.90. Because these between-side differences reflect genuine wear and loading asymmetry rather than measurement error, agreement was not used to exclude pairs. Hence, all 13 pairs of shoes were retained. These differences are small relative to the roughly two- to three-fold spread of each descriptor across the sample on which the subsequent analyses depend. Shoe #1 is the same high-leverage pair identified in the Results, where the leave-one-out analysis directly bounds its influence, so no reported correlation or component that survives that check depends on it.

The steel ball was seated in the heel cup of each shoe, where it settled under gravity into the lowest point of the cup, directly over the heel cushion. The shoe was then repositioned on the lower plate so that the ball, resting in the heel cup, was centered beneath the upper cylinder before each test. This kept the applied load balanced over the heel cushion and ensured the shoe and ball were seated securely so that neither could shift or eject during loading. Because the ball settled into the lowest point of the heel cup and the shoe was then centered consistently beneath the cylinder, the loading location was repeatable across shoes. The shoes spanned a limited size range, and the ball was fully seated in the heel cup of every shoe. Residual differences in heel-cup shape could introduce minor variation in the exact load location; this was not separately quantified, but a small offset is unlikely to alter the conclusion, since all shoe heels accommodated the ball.

Each pair was characterized by three geometric measurements, six conventional compression descriptors, four shoulder-point parameters, and one derived ratio; these four categories, are: (i) three geometric measurements comprised of heel height, toe height, and heel-to-toe drop; (ii) six conventional compression descriptors comprised of PC, E_{abs}, η, K_{low}, K_{mid}, and K_{high}; (iii) four shoulder-point parameters comprised of $(E/F)_{max}$, F_{opt}, x_{opt}, and E_{opt}; and (iv) one derived ratio, K_{mid}/K_{low}. The three geometric measurements and the six conventional descriptors are defined next, the four shoulder-point parameters in the following paragraph, and the derived ratio K_{mid}/K_{low} thereafter. Heel and toe heights and the heel to toe drop were measured with calipers while the shoe was not loaded (mm). Peak compression (PC, mm) was the amount the shoe compressed at the peak force of 4,500 N. Heel stiffness was calculated as the slope of the loading curve across three force ranges, each chosen to represent a different phase of impact: K_{low} (300 to 1,000 N) covered the initial low-load portion of the loading curve; K_{mid} (1,000 to 2,500 N) covered the mid-load range, which overlaps the first vertical ground-reaction-force peak of running that Fuss *et al.* report at approximately 0.7–2.0 kN (5);

and K_{high} (2,500 to 4,000 N) covered the high-load range, where the foam is expected to be stiffening toward densification (1). Absorbed energy (E_{abs}, J) was the area under the loading curve, calculated by integrating force over compression from zero to peak compression (at 4,500 N). Returned energy was the area under the unloading curve. Energy return efficiency (η, %) was the ratio of returned energy to absorbed energy.

The four shoulder point parameters were calculated following the method of Fuss *et al*. (5). At every sampled point along the loading curve, the energy absorbed up to that point was calculated the same way as E_{abs} but using that point's compression value as the upper limit instead of peak compression. This running energy value was then divided by the force at the same point. The maximum value of this running ratio was identified as the shoulder point, which produced the four parameters defined in the introduction: $(E/F)_{max}$, the peak value of the energy to force ratio (J/kN); F_{opt}, the force at the shoulder point (kN); x_{opt}, the compression at the shoulder point (mm); and E_{opt}, the energy absorbed up to the shoulder point (J). Each shoe's left and right loops were processed separately, and the average across the two sides is reported. From these parameters, the foam stiffening ratio K_{mid}/K_{low} was also calculated.

Statistical Analysis

Correlations between each of the four shoulder-point parameters and each of the six conventional descriptors, together with heel height and the derived foam-stiffening ratio K_{mid}/K_{low}, were computed across the 13 shoes using two different methods. Pearson correlation measures how closely two variables move together in a straight-line relationship. Spearman correlation measures how closely they move together in rank order, regardless of whether the relationship is linear. Both were reported because a high Pearson value combined with a low Spearman value would indicate that a small number of shoes were driving the linear relationship rather than a consistent pattern across the sample. For the key correlations, 95% confidence intervals were computed using the Fisher z-transformation (n = 13). Given the small sample, these intervals are wide and are reported to convey the uncertainty around each effect size rather than as precise estimates; the leave-one-out analysis described below serves as the primary check against any single shoe driving a result. The K_{mid}/K_{low} ratio was included specifically to test the prediction that F_{opt} tracks how quickly the foam stiffens out of its low-load range.

For each correlation, a leave-one-out (LOO) sensitivity check was also performed. The full correlation was recomputed 13 times, each time with one shoe removed, and the smallest absolute correlation value across these 13 subsamples was recorded as the LOO worst case. Pairs whose LOO worst case Pearson and Spearman values both remained at 0.75 or higher in absolute value were classified as LOO robust. Pairs whose LOO worst case values fell between 0.50 and 0.75 were classified as LOO moderate. Pairs whose full correlation exceeded 0.70 in absolute value but whose LOO worst case fell below 0.50 were classified as LOO fragile, meaning that the full correlation was being driven by one or two specific shoes rather than by a consistent pattern across the sample.

Because E_{opt} is the energy absorbed up to the force F_{opt}, both the total absorbed energy E_{abs} and the shoulder point force F_{opt} are natural predictors of E_{opt}. A linear regression of E_{opt} on E_{abs} and F_{opt} jointly was used to test whether E_{opt} could be predicted accurately from these two parameters combined.

Principal component analysis (PCA) was performed to identify the largest axes of variation across the sample. PCA is a method for taking a set of related measurements and finding the smallest number of underlying patterns that explain most of the variation in the data. Each descriptor was first standardized to have a mean of zero and a variance of one, and the analysis was performed using singular value decomposition of the standardized data matrix. Because the number of pairs of shoes (13) is small relative to the number of descriptors entered (10), the PCA is treated as an exploratory and descriptive summary of the variation within this sample rather than as a basis for inference about a component structure that would generalize to other samples. As with the correlations, a leave-one-out sensitivity check was also applied to the PCA, recomputing the component loadings and variance fractions across the 13 subsamples obtained by removing one pair at a time. Two variables that appeared in the correlation analysis were excluded from the PCA. Heel height was excluded because it is a geometric measurement rather than a descriptor calculated from the force compression loop and including it would mix two different kinds of measurements in the same analysis. The foam stiffening ratio K_{mid}/K_{low} was excluded because it is mathematically determined by K_{low} and K_{mid}, both of which were already included as separate variables, and including the ratio as well would count the same information twice. Heel height was retained in the pairwise correlation analysis to test whether the four shoulder point parameters were redundant with simple heel geometry, and K_{mid}/K_{low} was retained there to test the specific prediction that F_{opt} tracks how quickly the foam stiffens out of its low load range.

Ethical Considerations

This study was reviewed and approved by an institutional ethics review committee at Manlius Pebble Hill School, DeWitt, NY, comprised of a faculty research advisor, the Dean of Academics, and the school nurse, serving as the equivalent of an Institutional Review Board. Informed consent was obtained from all participants prior to data collection; since all participants were under 18, parental or guardian consent was obtained together with student consent. No sensitive, health-related, or personally identifiable information was collected, and each shoe was assigned a numeric identifier (Shoe #1–13) with no revealed link to the student who provided it.

RESULTS

Compression Behavior Across 13 Used Shoes

Each of the 13 athletic shoe pairs was tested on an Instron 5969 materials testing machine using a load-unload cycle to a peak force of 4,500 N at 600 mm per minute in both directions at 50 Hz. Each shoe was tested on both left and right heel, and the values reported here are the left–right pair mean (see Compression Testing for the between-side agreement supporting this averaging). Table 1 lists the heel and toe heights, the heel-to-toe drop, the six conventional compression descriptors (PC, E_{abs}, η, K_{low}, K_{mid}, K_{high}), the four shoulder point parameters ($(E/F)_{max}$, F_{opt}, x_{opt}, E_{opt}), and the foam stiffening ratio K_{mid}/K_{low}, for all 13 shoe pairs, sorted in order from least to most peak compression (PC).

Across the 13 pairs of shoes, peak compression varied by about 1.8 times, from 18.2 mm (Shoe #1, the firmest in the sample) to 33.4 mm (Shoe #13, the softest). Absorbed energy varied by about 1.9 times, from 19.4 J to 36.3 J, and was strongly correlated with peak compression (Pearson r = 0.93). Energy return efficiency η ranged from 30.3% to 58.0% with no obvious dependence on softness; several shoes with similar peak compression differed in energy return by more than 10 percentage points. Stiffness rose sharply with applied force in every shoe. The ratio of K_{high} to K_{low} ranged from 5.4 (Shoe #1) to 14.6 (Shoe #7), with a sample mean of 9.3, and K_{mid} was on average 2.9 times K_{low} (range 2.2 to 3.5).

The four shoulder point parameters also showed substantial spread across the sample. $(E/F)_{max}$ ranged from 4.52 to 9.58 J/kN, x_{opt} ranged from 15.5 to 27.4 mm, and E_{opt} ranged from 8.3 to 21.1 J. F_{opt} ranged from 1.32 to 3.28 kN. Two shoes fell outside the 0.7 to

Table 1. *Heel and toe geometry, the ten compression descriptors (six conventional and four shoulder-point), and the derived foam-stiffening ratio K_{mid}/K_{low} for each of the 13 used athletic shoes, sorted in ascending order of peak compression at 4,500 N.*

Shoe #	Heel (mm)	Toe (mm)	Drop (mm)	PC (mm)	E_{abs} (J)	η (%)	K_{low} (N/mm)	K_{mid} (N/mm)	K_{high} (N/mm)	K_{mid}/K_{low}	$(E/F)_{max}$ (J/kN)	F_{opt} (kN)	x_{opt} (mm)	E_{opt} (J)
1	28.3	19	9.2	18.2	19.4	40.9	156	353	847	2.26	4.52	3.28	17.1	15.5
2	30.9	29.7	1.2	20.3	22.6	30.3	103	278	792	2.70	5.82	1.59	15.5	9.3
3	44	30.6	13.4	21.5	23.3	44.4	101	267	742	2.64	5.69	1.92	17.4	10.9
4	29.6	19.7	9.9	23.4	21.3	52.5	88	303	1001	3.44	6.01	1.39	18.4	8.3
5	32.7	18.5	14.2	24.5	24.2	41.3	86	271	713	3.15	6.18	1.51	19	9.3
6	38.7	20.1	18.7	25	26	44.6	78	249	668	3.19	6.85	1.43	18.8	9.8
7	36.8	25.7	11.1	27	23.8	52.4	72	254	1050	3.53	7.4	1.32	21.3	9.7
8	43.8	30.1	13.7	28.9	28.5	57.6	66	195	791	2.95	8.46	1.61	23.3	13.6
9	30.8	20.7	10.1	29.5	29.9	53.4	77	190	616	2.47	7.95	1.81	24.1	14.4
10	46.1	38.7	7.4	32.1	34	58	62	165	555	2.66	9.32	1.8	26	16.8
11	39.8	30.9	9	32.2	36.3	49.9	71	154	452	2.17	9.25	2.29	27.4	21.1
12	42.6	29.5	13.1	33	32.7	55.4	58	173	623	2.98	9.43	1.63	26.5	15.4
13	41.2	20.4	20.8	33.4	32.2	55.8	57	176	665	3.09	9.58	1.56	26.8	14.9

2.0 kN F_{opt} band that Fuss *et al.* (5) identified as well designed for running heel strikes. Shoe #11 (F_{opt} = 2.29 kN) is classified as over designed under their scheme, and Shoe #1 (F_{opt} = 3.28 kN) is classified as excessively over designed. Both shoes are non-running shoes, so this classification reflects a category mismatch rather than a design flaw for the shoe's intended use. No shoes in the sample fell into the under designed range.

Correlations Among the Ten Compression Descriptors

Pearson and Spearman correlations were computed across the 13 shoes between each pair of the four shoulder point parameters and the six conventional descriptors. The foam stiffening ratio K_{mid}/K_{low} was also included as a column to test the prediction described in the introduction that F_{opt} tracks how quickly the foam stiffens out of its low load range. For every correlation, the leave one out (LOO) worst case was also computed across the 13 subsamples obtained by removing one shoe pair at a time. Table 2 lists the full Pearson and Spearman values, the LOO worst case values, and the LOO classification (green = robust, amber = moderate, coral = fragile) for every shoulder point parameter against every conventional descriptor. The between-side agreement of the pair-mean values entering these correlations is reported in Table 3 (mean absolute left–right difference and ICC(2,1) for each descriptor).

Two of the four shoulder point parameters, $(E/F)_{max}$ and x_{opt}, produced LOO robust correlations with several conventional descriptors. This means each correlation remained strong even when any single shoe was removed from the sample, indicating that the association reflects a consistent pattern across all 13 shoes rather than the influence of one or two specific shoes.

$(E/F)_{max}$ was nearly indistinguishable from peak compression. The full Pearson and Spearman values were both above 0.98 (Pearson r = 0.99, 95% CI (0.96, 1.00); r^2 = 0.97, i.e. 97% shared variance), and the LOO worst case values stayed above 0.97 for both methods. $(E/F)_{max}$ also produced LOO robust correlations with K_{mid} (r = -0.96, ρ = -0.90), K_{low} (r = -0.87, ρ = -0.98), and absorbed energy (r = 0.94, ρ = 0.90). Because the Spearman correlation between $(E/F)_{max}$ and peak compression was 0.98 in the full sample and 0.98 in the LOO worst case, the rank order of shoes by $(E/F)_{max}$ is essentially identical to the rank order by peak compression, and this near identity does not depend on any single shoe in the sample.

x_{opt} showed the same pattern. Its Pearson and

Table 2. *Pearson r, Spearman ρ, and leave-one-out (LOO) worst-case Pearson and Spearman correlations between each shoulder point parameter (rows) and each conventional compression descriptor, plus the derived foam-stiffening ratio K_{mid}/K_{low} (columns) across the 13 shoes. Cell shading: green = LOO-robust (both LOO|r| ≥ 0.75); amber = LOO-moderate; coral = LOO-fragile (full |r| > 0.7 but LOO collapses below 0.5).*

Shoulder point↓ conventional parameter →	Heel	PC	E_{abs}	η	K_{low}	K_{mid}	K_{high}	K_{mid}/K_{low}
$(E/F)_{max}$	r = 0.66 ρ=+0.55 LOO: +0.57 / +0.43	r = 0.99 ρ=+0.98 LOO: +0.98 / +0.98	r = 0.94 ρ=+0.90 LOO: +0.93 / +0.87	r = 0.75 ρ=+0.81 LOO: +0.72 / +0.78	r = -0.87 ρ=-0.98 LOO: -0.86 / -0.98	r = -0.96 ρ=-0.90 LOO: -0.95 / -0.87	r = -0.58 ρ=-0.66 LOO: -0.51 / -0.61	r = 0 ρ=+0.06 LOO: -0.00 / +0.01
F_{opt}	r = -0.23 ρ=+0.15 LOO: -0.21 / +0.04	r = -0.3 ρ=+0.02 LOO: -0.28 / -0.01	r = -0.11 ρ=+0.22 LOO: -0.07 / +0.05	r = -0.23 ρ=-0.07 LOO: +0.06 / +0.00	r = 0.71 ρ=+0.09 LOO: -0.03 / -0.00	r = 0.28 ρ=-0.24 LOO: +0.26 / -0.08	r = -0.18 ρ=-0.46 LOO: -0.04 / -0.31	r = -0.79 ρ=-0.97 LOO: -0.77 / -0.96
x_{opt}	r = 0.57 ρ=+0.48 LOO: +0.50 / +0.36	r = 0.97 ρ=+0.97 LOO: +0.97 / +0.97	r = 0.94 ρ=+0.93 LOO: +0.93 / +0.91	r = 0.79 ρ=+0.72 LOO: +0.75 / +0.64	r = -0.74 ρ=-0.91 LOO: -0.71 / -0.90	r = -0.91 ρ=-0.92 LOO: -0.90 / -0.90	r = -0.6 ρ=-0.74 LOO: -0.51 / -0.66	r = -0.14 ρ=-0.10 LOO: -0.06 / -0.02
E_{opt}	r = 0.38 ρ=+0.40 LOO: +0.28 / +0.26	r = 0.6 ρ=+0.55 LOO: +0.54 / +0.48	r = 0.76 ρ=+0.65 LOO: +0.66 / +0.55	r = 0.42 ρ=+0.40 LOO: +0.31 / +0.27	r = -0.18 ρ=-0.49 LOO: -0.12 / -0.40	r = -0.63 ρ=-0.68 LOO: -0.54 / -0.60	r = -0.71 ρ=-0.67 LOO: -0.59 / -0.58	r = -0.71 ρ=-0.68 LOO: -0.58 / -0.60

Table 3. *Between-side (left–right) agreement across the 13 shoe pairs. For each descriptor: the mean absolute percent difference between the left and right values, and the absolute agreement intraclass correlation coefficient ICC(2,1) with its 95% confidence interval. The ICC is the fraction of a descriptor's total variance that lies between shoes rather than between the two sides of a shoe; values near 1 indicate the left–right mean is a reliable summary of the pair.*

Category	Parameter	Mean |L−R| (%)	ICC(2,1) [95% CI]
Conventional	Peak compression (PC)	4.4	0.96 [0.86, 0.99]
Conventional	Absorbed energy (E_{abs})	10.6	0.84 [0.60, 0.95]
Conventional	Energy return efficiency (η)	8.6	0.76 [0.38, 0.92]
Conventional	Low-load stiffness (K_{low})	8.2	0.94 [0.79, 0.98]
Conventional	Mid-load stiffness (K_{mid})	16	0.78 [0.46, 0.94]
Conventional	High-load stiffness (K_{high})	12.6	0.75 [0.38, 0.93]
Shoulder point	$(E/F)_{max}$	11.8	0.86 [0.62, 0.96]
Shoulder point	F_{opt}	9.9	0.64 [0.20, 0.88]
Shoulder point	x_{opt}	4.8	0.96 [0.88, 0.99]
Shoulder point	E_{opt}	18.2	0.57 [0.12, 0.86]
Derived ratio	K_{mid}/K_{low} ratio	12.7	0.44 [-0.08, 0.79]

Spearman correlations with peak compression were 0.97 and 0.97, both LOO robust (Pearson 95% CI (0.91, 0.99); $r^2 = 0.95$). A linear fit showed that x_{opt} was approximately 80% of peak compression across the sample (mean x_{opt} / PC across Shoes #2 through #13 was 0.81 ± 0.04). Shoe #1 was the lone outlier at 0.94, which is consistent with that shoe's broader mechanical behavior discussed below.

F_{opt} showed the opposite pattern. Its Spearman correlations with every conventional descriptor were 0.46 or smaller in absolute value, and most were close to zero. Specifically, F_{opt} against peak compression was $\rho = 0.02$, against absorbed energy was $\rho = 0.22$, against energy return efficiency was $\rho = -0.07$, against K_{low} was $\rho = 0.09$, against K_{mid} was $\rho = -0.24$, and against K_{high} was $\rho = -0.46$. F_{opt} was also uncorrelated in rank order with the other shoulder point parameters $(E/F)_{max}$ ($\rho = -0.04$) and x_{opt} ($\rho = 0.12$). In other words, knowing any of the conventional descriptors or either of the other two shoulder point parameters tells you essentially nothing about F_{opt}, and vice versa.

The one apparent exception was the Pearson correlation between F_{opt} and K_{low} ($r = 0.71$), which would otherwise suggest a moderate linear relationship. However, this correlation was driven entirely by the firmest shoe in the sample (Shoe #1, with F_{opt} = 3.28 kN and K_{low} = 156 N/mm). When Shoe #1 was removed from the analysis, the Pearson correlation collapsed to $r = -0.03$. The corresponding Spearman correlation was only $\rho = 0.09$ in the full sample, indicating that no consistent rank order relationship exists. The F_{opt}-K_{low} Pearson value is therefore classified as LOO fragile in Table 2 (coral shading) and is likely not a genuine association. Notably, the full-sample 95% confidence interval for this correlation ((0.27, 0.91)) excludes zero, yet the interval is an artifact of a single high-leverage shoe; this case illustrates why confidence intervals are reported alongside Spearman and leave-one-out values rather than interpreted on their own.

F_{opt} was also tested against the foam stiffening ratio K_{mid}/K_{low}, to access the prediction given in the introduction. Across the 13 shoes, this ratio varied from 2.17 to 3.53. F_{opt} and the stiffening ratio correlated at Pearson $r = -0.79$ and Spearman $\rho = -0.97$ (95% CI (−0.93, −0.42) for r; $r^2 = 0.62$), with a LOO worst case Spearman of -0.96 across all 13 removals. This was the strongest single correlation involving F_{opt} anywhere in the analysis. The ratio K_{mid}/K_{low} has the weakest between-side agreement of any descriptor (ICC of 0.44, confidence interval including zero), as expected for a quotient of two separately fitted stiffness slopes, whose compounded noise makes the ratio inherently less reliable than either slope alone. This low single-side reliability does not undermine the relationship, which holds separately for each side ($\rho = -0.86$ left, −0.94 right) and is strongest for the left–right average (ρ = −0.97). The low ICC shows that a pair's two sides can differ, and that scatter weakens each side's correlation on its own; averaging cancels part of it, so the averaged ratio correlates more strongly.

The negative direction of the correlation can be interpreted straightforwardly. A shoe with a high F_{opt} is one whose mid-load stiffness is only modestly greater than its low load stiffness, while a shoe with a low F_{opt} is one whose mid load stiffness rises steeply over its low load stiffness. In other words, F_{opt} is high when the foam stiffens gradually and low when the foam stiffens sharply.

The Pearson value (-0.79) is smaller in absolute value than the Spearman value (-0.97) because the underlying relationship is monotonic but not linear. Figure 1c shows F_{opt} decreasing with K_{mid}/K_{low} along a curved trajectory that a straight line captures only approximately. Figure 1 shows the three most informative scatter relationships in the analysis: panels (a) and (b) illustrate the near redundancy of $(E/F)_{max}$ and x_{opt} with peak compression, and panel (c) shows the F_{opt} against stiffening ratio relationship.

E_{opt} occupied an intermediate position between the redundant parameters $(E/F)_{max}$ and x_{opt} and the independent parameter F_{opt}. Its correlations with conventional descriptors were moderate rather than strong. E_{opt} against absorbed energy had Pearson r = 0.76 and Spearman ρ = 0.65, with a LOO worst case Pearson of 0.66. E_{opt} against K_{high} had r =- 0.71, ρ = -0.67, and a LOO worst case Pearson of -0.59. The strongest rank correlation for E_{opt}, however, was with F_{opt} itself (Spearman ρ = 0.75, LOO worst case ρ = 0.69), meaning E_{opt} was more strongly rank-correlated with another shoulder point parameter than with any conventional descriptor. The Spearman 95% confidence interval for this relationship was (0.26, 0.93); the corresponding Pearson interval included zero ((−0.00, 0.85), p = 0.05), consistent with a monotonic but non-linear association.

To test whether E_{opt} can be jointly captured by E_{abs} and F_{opt}, a multiple linear regression of E_{opt} on E_{abs} and F_{opt} was performed. The two predictors together accounted for 98.1% of the variance in E_{opt} (adjusted R^2 = 0.978, $p < 0.001$; residual standard deviation 0.57 J). The fitted model was $E_{opt} = -11.26 + 0.585 \cdot E_{abs} + 4.68 \cdot F_{opt}$ (E_{opt} and E_{abs} in J, F_{opt} in kN). Both predictors were highly significant: the E_{abs} coefficient was 0.585 (95% CI (0.517, 0.653), $p < 0.001$) and the F_{opt} coefficient was 4.68 (95% CI (3.97, 5.38), $p < 0.001$). When the variables were standardized so the two predictors could be compared directly, both contributed substantially, with the absorbed

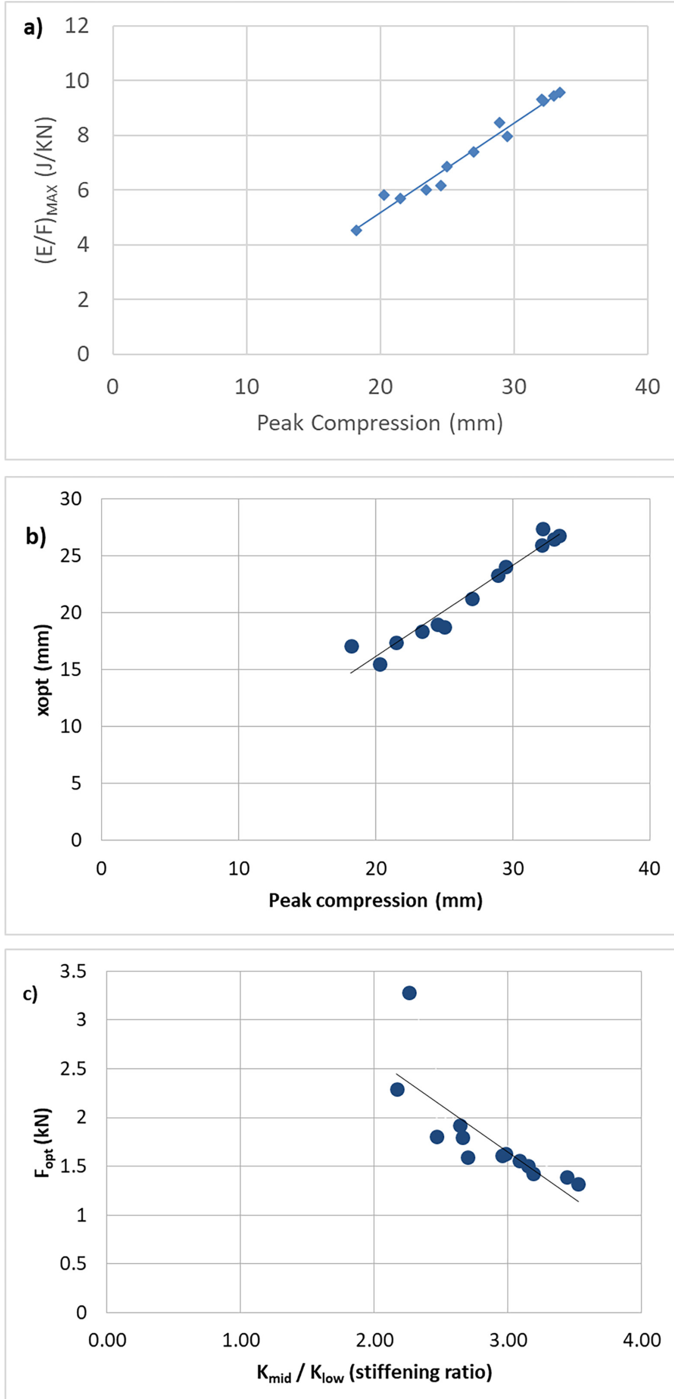

Figure 1. *Three illustrative scatter relationships across 13 shoes. (a) (E/F)max plotted against peak compression: the two are essentially linearly related and rank-equivalent (Spearman ρ = 0.98). (b) x_{opt} plotted against peak compression: the same near-linear and rank-equivalent relationship (ρ = 0.97). (c) F_{opt} plotted against the K_{mid}/K_{low} foam-stiffening ratio shows a strong negative rank-correlation (ρ = −0.97) that no conventional descriptor produces against the same axis. Lines are best linear fits.*

energy predictor carrying somewhat more weight than the shoulder point force (standardized $\beta = 0.83$ for E_{abs} and 0.64 for F_{opt}). By comparison, absorbed energy alone accounted for 57.8% of E_{opt}'s variance in the full sample. The joint model itself, however, was insensitive to single-shoe removal: across the 13 leave-one-out subsamples its R^2 ranged only from 0.971 to 0.986 (0.981 with Shoe #1 removed), and the F_{opt} coefficient remained positive and significant throughout (4.38, 95% CI (2.46, 6.30), $p < 0.001$ with Shoe #1 removed). E_{opt} is therefore not an independent shoulder point parameter in this sample. Rather, it is well described as a near linear combination of one conventional descriptor (E_{abs}) and one shoulder point descriptor (F_{opt}). This pattern suggests that E_{opt} and F_{opt} together describe a portion of the descriptor space that captures both the overall magnitude of energy absorption and the shape and a portion of the loading curve.

To test whether the four shoulder point parameters were redundant with simple heel geometry, heel height was added to the correlation analysis as an additional variable. Across the 13 shoes, heel height correlated moderately with $(E/F)_{max}$ (Pearson $r = 0.66$, Spearman $\rho = 0.55$) and with x_{opt} ($r = 0.57$, $\rho = 0.48$), weakly with E_{opt} ($r = 0.38$, $\rho = 0.39$), and was essentially uncorrelated with F_{opt} ($r = -0.23$, $\rho = 0.15$). The inconsistent sign between the Pearson and Spearman values for the F_{opt} correlation further indicates that no real relationship exists between F_{opt} and heel height in this sample. All four of these correlations fell below the LOO robust and LOO moderate thresholds, with LOO worst case Spearman values ranging from 0.04 (for F_{opt}) to 0.43 (for $(E/F)_{max}$). None of the four shoulder point parameters is therefore redundant with heel height.

These correlations are weaker than the R^2 values above 0.92 that Fuss *et al.* (5) reported between three of the four shoulder point parameters and stack height. Two factors explain the difference. First, their correlations were computed across six shoe models chosen specifically to span the full minimalist-to-maximalist range, which maximizes the variation in stack height. The 13 shoes in the present sample spanned only 28 to 46 mm in heel height, with no minimalist or racing shoes included. Second, heel height is not the same quantity as total stack height. The lower correlations reported here therefore describe a natural mid-range sample rather than contradicting the Fuss *et al.*'s (5) findings. Notably, F_{opt}'s lack of association with heel height ($r = -0.23$) is consistent with their finding that F_{opt} does not correlate with stack height ($R^2 < 0.46$).

Principal Component Analysis of the Shoe Descriptors

Principal component analysis was applied to the ten compression descriptors to estimate how many independent dimensions of variation exist across the sample. The method combines the original descriptors into a smaller set of summary variables called principal components, with the first principal component capturing the largest direction of variation across shoes, the second capturing the next largest direction independent of the first, and so on. To allow descriptors measured in different units to be combined on a common scale, each descriptor was first standardized to have a mean of zero and a variance of one before the analysis. Figure 2 shows the resulting biplot of the 13 shoes projected onto the first two principal components, together with the variable loadings that are shown as arrows whose direction and

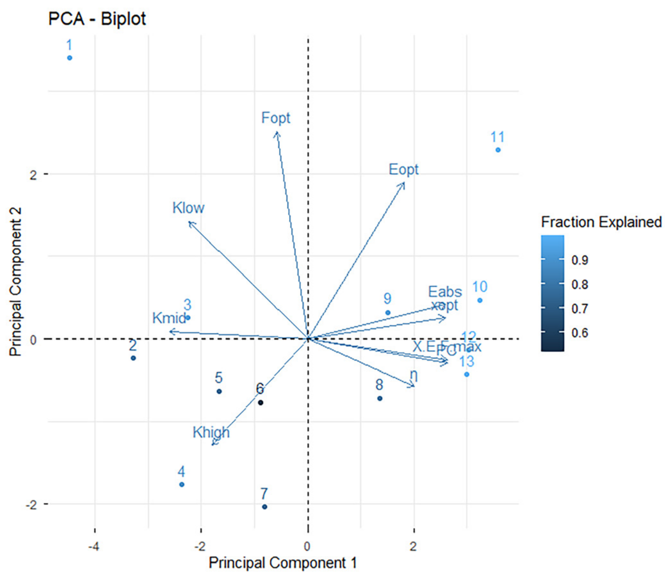

Figure 2. *Principal-component (PC) biplot of the 13 shoes in the standardized ten-descriptor space. Each filled circle is one shoe, plotted at its (PC1, PC 2) score. The PC1 axis (horizontal) captures softness.* F_{opt} *and* E_{opt} *load most strongly on PC2 (vertical) at +0.66 and +0.50 respectively, with smaller contributions from* K_{low} *(0.38) and* K_{high} *(−0.34); the opposing signs of* K_{low} *and* K_{high} *indicate that PC 2 represents the contrast between low-load and high-load stiffness rather than stiffness magnitude, defining a secondary axis of variation orthogonal to softness. Circle shading indicates the percentage of each shoe's squared distance from the origin in the full 10-dimensional descriptor space that is preserved in the PC 1– PC 2 projection, with brighter shading denoting shoes whose mechanical signature is more fully captured in two dimensions. Across the sample, PC 1 and PC 2 jointly account for 90.4% of total variance.*

length indicate each descriptors contribution to each component. Figure 3 shows the scree plot and the full loadings table.

The first principal component (PC1) accounted for 70.3% of the variance across the ten standardized descriptors. PC1 weighs the eight softness- and cushioning-related descriptors with similar magnitude (|loading| ≈ 0.25 to 0.37). The four measures that increase with shoe softness, peak compression, absorbed energy, $(E/F)_{max}$, and x_{opt}, have positive loadings; the three stiffness measures K_{low}, K_{mid}, and K_{high} have negative loadings; and η and E_{opt} also have positive loadings. F_{opt} is the only descriptor with a near-zero loading on PC1 (−0.08), consistent with its independence from the softness axis. This loading pattern identifies PC1 as a softness axis. The firmer shoes (Shoes #1, #2, #3, #4) score negatively on PC1, while the softer shoes (Shoes #10, #11, #12, #13) score positively.

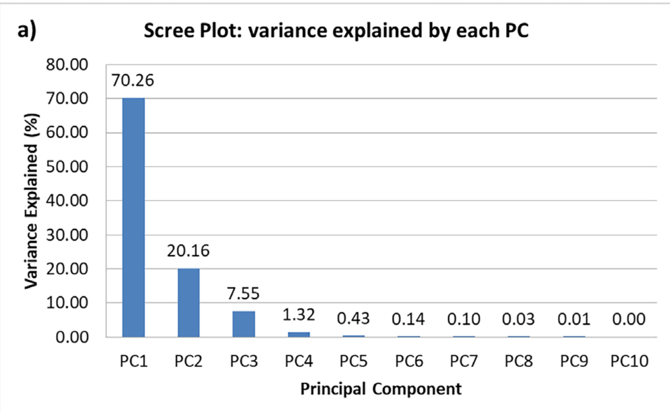

b) Loadings on PC1, PC2, PC3

Metric	PC1	PC2	PC3
PC	0.372	-0.078	0.075
E_{abs}	0.368	0.109	-0.167
η	0.285	-0.152	0.657
K_{low}	-0.315	0.376	0.125
K_{mid}	-0.369	0.024	0.170
K_{high}	-0.254	-0.341	0.590
$(E/F)_{max}$	0.372	-0.067	0.033
F_{opt}	-0.083	0.664	0.284
x_{opt}	0.367	0.067	0.194
E_{opt}	0.257	0.501	0.150

Figure 3. *(a) Scree plot showing the percentage of variance explained by each of the ten principal components. Three components account for 98.0% of variance across the sample. (b) Loadings of the ten descriptors on the first three principal components. PC1 (70.3%) is a softness axis; PC2 (20.2%) is loaded primarily by F_{opt} and E_{opt} with a secondary emphasis on difference in K_{high} and K_{low}; PC3 (7.6%) is loaded by η and K_{high}.*

The second principal component (PC2) accounted for an additional 20.2% of the variance and was dominated by F_{opt} (loading 0.66) and E_{opt} (0.50), with smaller contributions from K_{low} (0.38) and K_{high} (-0.34). The opposite signs and similar magnitudes of the K_{low} and K_{high} loadings indicate that PC2 is picking up a contrast between the two stiffness ranges rather than their overall magnitude: a shoe scores high on PC2 when its low load stiffness is high relative to its high load stiffness, which is the same pattern as a shoe with a high F_{opt}. The conventional descriptors $(E/F)_{max}$, x_{opt}, and peak compression loaded near zero on PC2. PC2 is therefore a dimension orthogonal to softness, defined jointly by F_{opt} and E_{opt}. F_{opt} remained the dominant loading on PC2 in all 13 leave-one-out subsamples, so the second axis itself does not depend on any single shoe. The contribution of E_{opt} to this axis was less stable. Removing the firmest pair (Shoe #1) from the PCA analysis roughly halved the PC2 loading of E_{opt} (from 0.50 to 0.23), whereas the PC2 loading of F_{opt} remained dominant (0.66 to 0.58). These are the same two shoulder point parameters that were most weakly correlated with the conventional descriptors in the bivariate analysis, confirming that they capture variation the conventional descriptors do not.

The third principal component (PC3) accounted for 7.6% of the variance and was dominated by energy return efficiency η (loading 0.66) and K_{high} (0.59). PC3 is an axis combining energy return and high-load stiffness. Shoes at the positive end tend to combine high energy return with elevated high-load stiffness. One interpretation is that in these shoes the high-load resistance comes from compressing dense, elastic cell walls, which is recoverable and returns energy, rather than from dissipative cell collapse (1). Under this interpretation, the foam stiffens enough to help protect the foot from bottoming out while still returning the stored energy during push off (3). Shoes #4, #7, and #8 sit at the positive end of this axis, each with energy return efficiency above 52% and K_{high} above 790 N/mm. Shoe #2, at the negative end, shows that these two properties need not coincide: it has the lowest energy return efficiency in the sample (30.3%) despite an above-average K_{high}.

Because the biplot in Figure 2 shows the 13 shoes projected onto only the first two principal components, some information about each shoe's position in the full ten-dimensional descriptor space is necessarily lost. To quantify how well each shoe is represented in this two-dimensional view, the fraction of each shoe's squared distance from the origin that survives the projection onto the PC1-PC2 plane was computed. A value near 1.0 means the shoe's position is captured almost entirely by PC1 and PC2, while a lower value means a substantial portion of that shoe's distinctiveness lies along PC3 or higher components. Across the 13 shoes, this fraction ranged from 51.7% (Shoe #6) to 99.4% (Shoe #12). The softest maximalist shoes (Shoes #10, #11, #12, #13) were each represented at 97% or above, and the firmest shoe in the sample (Shoe #1) was represented at 95.2%, indicating that shoes at the extremes of softness vary almost entirely along the PC1-PC2 plane and are well captured by the two-dimensional biplot. The mid sample shoes (Shoes #5, #6, #7, #8) were less completely captured, with representations between 52% and 76%. The variation these shoes carry that the PC1-PC2 plane misses lies primarily on PC3, the axis along which energy return efficiency η and K_{high} covary.

PC1, PC2, and PC3 together accounted for 98.0% of the total variance across the ten descriptors. This indicates that the ten compression descriptors are well described by approximately three independent dimensions across this 13-shoe sample. Two of these three dimensions are defined by conventional descriptors: PC1 is a softness axis, and PC3 is an energy return and high-load axis. The remaining dimension, PC2, is defined by the shoulder point parameters F_{opt} and E_{opt}. Of these two, F_{opt} is the parameter whose loading on this axis is robust to single-shoe removal. The shoulder point framework therefore contributes a direction of variation in the descriptor space that the conventional measurements do not.

DISCUSSION

Of the four shoulder point parameters proposed by Fuss *et al*. (5), two behaved very differently from the other two when applied to 13 used athletic shoes. In this sample, $(E/F)_{max}$ and x_{opt} provided essentially the same ranking as peak compression, suggesting that in datasets with similar characteristics they may add little beyond peak compression and could be treated as consistency checks rather than independent descriptors. Whether this redundancy holds across larger and more varied samples remains to be tested. F_{opt} and E_{opt}, in contrast, carried information that the conventional descriptors did not.

F_{opt} was uncorrelated in rank with every conventional descriptor and instead tracked the foam stiffening ratio K_{mid}/K_{low} strongly and robustly. This independence from conventional compression descriptors is consistent with Fuss *et al.*'s finding (5) that F_{opt} does not correlate with stack height, the only conventional geometric descriptor they tested against the shoulder point parameters. The two studies provide cross sample support for F_{opt} as a parameter that captures information not contained in conventional descriptors.

E_{opt} did not produce strong correlations with any conventional descriptor on its own, but a regression of E_{opt} on absorbed energy and F_{opt} accounted for 98.1% of its variance. E_{opt} is therefore not an independent shoulder point parameter in this sample, but neither is it a function of conventional descriptors alone. It is well described as a near linear combination of one softness descriptor (E_{abs}) and one shoulder point descriptor (F_{opt}). In the principal component analysis, F_{opt} and E_{opt} jointly defined PC2, an axis independent of both the softness axis (PC1) and the energy return and high-load axis (PC3).

The hypothesis that not all four shoulder point parameters carry independent information beyond conventional compression descriptors is therefore supported. A more refined statement of the finding is that, in this sample, the shoulder point framework contributes one new dimension to the descriptor space rather than four, and that F_{opt} and E_{opt} jointly describe this dimension.

The mechanical interpretation of the F_{opt} and K_{mid}/K_{low} relationship is consistent with how the shoulder point is defined. The shoulder point is the compression at which the running ratio of absorbed energy to applied force is at its maximum (5). Before the shoulder, the foam is in its low load range, where additional compression produces relatively more absorbed energy than additional force, so the ratio is rising. After the shoulder, the foam has entered the high load and densification range (1), where additional compression produces relatively more force than additional energy, so the ratio is falling. The shoulder therefore marks the transition between these two ranges, and the force at which the transition occurs (F_{opt}) depends on how steeply the foam stiffens out of its low load range.

A shoe whose foam stiffens steeply between 1,000 N and 2,500 N (high K_{mid}/K_{low}) will reach the shoulder at a comparatively low force, because the foam is rapidly leaving its most compliant range. A shoe whose foam stiffens gradually (low K_{mid}/K_{low}) will continue to absorb energy efficiently for longer along the force axis and will therefore reach the shoulder at a comparatively higher force. The strong negative correlation between F_{opt} and K_{mid}/K_{low} across the 13 shoes captures exactly this relationship. F_{opt} is a force domain summary of curve shape that no individual conventional descriptor reports.

The intermediate behavior of E_{opt} has a similar mechanical interpretation. E_{opt} is the cumulative energy absorbed up to the shoulder point, which depends on two things: how much energy the shoe absorbs overall (scaling with absorbed energy) and how far up the force axis the shoulder sits (scaling with F_{opt}). The high R^2 of the joint regression on absorbed energy and F_{opt} (98.1%) quantifies this two-factor structure. E_{opt} rank-correlated more strongly with F_{opt} ($\rho = 0.75$) than with absorbed energy ($\rho = 0.65$) consistent with shoes whose shoulders sit at higher forces accumulating more energy on the way to those forces. E_{opt} is not an independent shoulder point parameter in this sample, but neither is it simply a proxy for absorbed energy: it is the joint product energy absorption (E_{abs}) and curve shape (F_{opt}), loading on the same principal component as F_{opt} (PC2).

The principal component analysis quantifies the implication for the descriptor space. The ten compression descriptors used to characterize these worn athletic shoes occupy approximately three independent dimensions of variation. One of those dimensions, the F_{opt} and E_{opt} axis, is contributed by the shoulder point framework rather than by any conventional descriptor. The secondary K_{low} and K_{high} loadings on this axis, with opposite signs and similar magnitudes, do not contradict this claim: they capture the same foam stiffening shape that F_{opt} measures directly, rather than contributing independent conventional information. The other two dimensions are defined by conventional descriptors: the softness axis (PC1), and the energy return, η, and high-load axis, K_{high}, (PC3) that distinguishes mid softness shoes by how cleanly their foams return energy at high load rather than by their overall softness.

Several caveats temper these conclusions. The 13 shoe pairs were drawn from a convenience sample of high school students and represent a range of athletic shoe categories (running, basketball, lifestyle, maximalist cushion) and a range of wear levels in active use. Wear was not formally characterized, and the shoes represent a range of conditions typical of in-use athletic footwear rather than a controlled wear representation. The correlations and LOO classifications reported here describe the variation across the sample as obtained. They should not be extrapolated to the full population of used athletic shoes, and they should not be interpreted as estimates of how each parameter changes with wear within a single shoe. The effect sizes reported here (the correlation coefficients, their shared variance, and the regression R^2) are large, but their precision is limited by the small sample, and the corresponding 95% confidence intervals are correspondingly wide. The intervals are consistent with the qualitative conclusions drawn here rather than providing precise estimates, and the leave-one-out analysis remains the primary safeguard against single-shoe leverage.

The compression test protocol is quasi-static (600 mm per minute), while a real impact loads the midsole much faster. Fuss *et al.* (5) reported that the shoulder point parameters are relatively insensitive to velocity across a range spanning more than one order of magnitude, which supports comparing the quasi-static results obtained here to dynamic shoe behavior. However, the absolute calibration between bench-measured stiffness and in-shoe stiffness during a landing remains approximate (3).

The principal component analysis quantifies dimensionality in this 13-shoe sample only. With ten descriptors entered against thirteen observations, the observation-to-variable ratio is low, and the precise loadings and variance fractions should not be regarded as stable estimates of a population structure. The qualitative result that matters for the conclusions, that F_{opt} loads on an axis separate from the softness descriptors, does not depend on this fine structure: it is independently corroborated by the pairwise correlations, which show the same separation without relying on the dimensionality of the full descriptor set. A larger sample, or a different shoe-category mix, could reveal additional dimensions of variation that this sample does not span. The placement of E_{opt} on this axis was itself less robust: in the leave-one-out sweep, removing the single firmest pair (Shoe #1) roughly halved the loading of E_{opt} on the second component, whereas the centrality of F_{opt} for that component was unaffected. This is consistent with the lower between-side agreement of E_{opt} (Table 3), and it is why the regression of E_{opt} on E_{abs} and F_{opt}, rather than its component loading, is treated here as the primary evidence for the structure of E_{opt}.

Only one load and unload cycle was used to compute the shoulder point parameters in this study, whereas Fuss *et al.* (5) recommended at least five separate tests per shoe at least 24 hours apart and reported the fifth cycle of each test. They observed that parameter values are larger in the first cycle than in later cycles, with the difference declining to about 1% by the fourth cycle. Across multiple days, they reported test to test variation of 2 to 6% depending on the parameter. The values reported here may therefore be both systematically elevated and noisier than five test averages would be. The relative ordering of the shoes is nonetheless expected to remain largely preserved across these limitations, because the first cycle effect is systematic across shoes and because the 2 to 6% test to test variation is small relative to the across shoe range for each parameter, which spans roughly two to three times across the 13 shoes.

One practical implication follows for how athletic shoes are described in the biomechanics literature. When the shoulder point framework is applied alongside conventional compression descriptors, reporting all four shoulder point parameters as if they were independent overstates the information content of the analysis. In a sample like this one, $(E/F)_{max}$ and x_{opt} provide essentially the same ranking as peak compression and could reasonably be omitted or reported only as a check on consistency. F_{opt} and E_{opt} are the parameters that add genuinely new information, jointly defining a single secondary axis of variation. Reporting F_{opt} and E_{opt} together with peak compression and absorbed energy captures most of the descriptor space observed across used athletic shoes.

CONCLUSION

This study tested whether the four shoulder point parameters proposed by Fuss *et al*. (5) carry information not already captured by conventional compression descriptors when applied to used athletic shoes. Thirteen used athletic shoes from a convenience sample of high school students were characterized by a materials testing machine, and the relationships among ten compression descriptors were analyzed.

Two of the four shoulder point parameters, $(E/F)_{max}$ and x_{opt}, were largely redundant with peak compression. The other two, F_{opt} and E_{opt}, carried information that no conventional descriptor reports directly. F_{opt} tracked the foam stiffening ratio K_{mid}/K_{low} strongly and robustly across the sample, identifying it as a force domain summary of curve shape. E_{opt} was well described as a near linear combination of absorbed energy and F_{opt}. In a principal component analysis, F_{opt} and E_{opt} jointly defined the second principal component, an axis independent of both the conventional softness axis and the conventional energy return and high-load axis. The shoulder point framework therefore contributes one new dimension to the conventional descriptor space rather than four.

These findings come from a convenience sample of 13 used shoes spanning a range of athletic categories and wear levels, characterized using a single quasi-static load and unload cycle. The relative ordering of the shoes is expected to be robust to these limitations, but the specific magnitudes reported here may not generalize to larger samples or to dynamic loading conditions.

F_{opt} is identified as a candidate parameter for tracking wear-induced changes in midsole behavior in future studies that compare matched new and worn shoes. Because F_{opt} tracks the K_{mid}/K_{low} ratio strongly, the direction of any wear-induced shift in F_{opt} would depend on the relative aging rates of low load and mid load stiffness. Paired new and used measurements of the same shoe models could directly address this question. If K_{low} rises faster with wear than K_{mid} does, F_{opt} would rise. If K_{low} and K_{mid} rise proportionally, F_{opt} would remain unchanged. If K_{mid} rises faster than K_{low}, F_{opt} would fall.

Of the four shoulder point parameters, F_{opt} is the most informative in this sample of used athletic shoes, and these results identify it as the parameter most likely to add value to future studies of how athletic shoe cushioning changes as the shoe is used. Because these observations come from a convenience sample of 13 shoes, they should be regarded as preliminary and warrant confirmation in larger and more diverse datasets.

FUNDING SOURCES

This work received no external funding.

CONFLICT OF INTEREST

The authors declare no conflicts of interest related to this work.

REFERENCES

1. Gibson LJ, Ashby M. The Structure of Cellular Solids. In: Cellular Solids: Structures and Properties. 2nd ed. Cambridge University Press. 1997; pp. 15-50. ISBN: 978-0-521-49911-8
2. ASTM F1976-24: Standard Test Method for Impact Attenuation of Athletic Shoe Cushioning Systems and Materials. Available from: https://store.astm.org/f1976-24.html (accessed on 2026-5-25)
3. Shorten, M. Energy Return in Footwear - Revisited. *Footwear Sci*. 2024; 16 (3): 149-162. https://doi.org/10.1080/19424280.2024.2369995
4. Even-Tzur, N. *et al*. Role of EVA Viscoelastic

Properties in the Protective Performance of a Sport Shoe: Computational Studies. *Bio-Med Mater and Eng*. 2006; 16 (5): 289-299.

5. Fuss FK, *et al*. A New Method and Set of Parameters for Evaluating the Cushioning Effect of Shoe Heels, Revealing the Inadvertent Design of Running Shoes. *Bioengineering*. 2025; 12 (5): 467-508. https://doi.org/10.3390/bioengineering12050467
6. Chambon, N *et al*. Aging of Running Shoes and its Effect on Mechanical and Biomechanical Variables: Implications for Runners. *J Sports Sci*. 2014; 32 (11): 1013-1022. https://doi.org/10.1080/02640414.2014.886127
7. Shrout, P.E., Fleiss, J.L. Intraclass Correlations: Uses in Assessing Rater Reliability. *Psychol Bull*. 1979; 86 (2): 420-428. https://doi.org/10.1037/0033-2909.86.2.420